EurJIC
European Journal of Inorganic Chemistry

Full Papers
doi.org/10.1002/ejic.202100380

Chemistry Europe
European Chemical Societies Publishing

Dendrimeric and Corresponding Monometallic Iridium(III) Catalysts Bound to Carbon Nanotubes Used in Hydroamination Transformations

Indrek Pernik[+],*[a, b] Antonin Desmecht[+],[c] Barbara A. Messerle,[b, d] Sophie Hermans,*[c] and Olivier Riant*[c]

This report describes the synthesis of a carbon nanotube-bound dendrimer and three carbon nanotube-bound monometallic complexes and their use as catalysts. The polyamidoamine third generation dendrimer used here incorporates pyrazole-triazole moieties suitable for ligating iridium(III) centres. The monometallic complexes use the same pyrazole-triazole ligands coordinated to an iridium(III) centre. All catalysts were characterized using ICP-AES and XPS to evaluate their metal loadings on the carbon surface with significantly higher relative weight percentage of iridium determined for the denrimeric species. The catalytic activity and practicality of the formed catalysts were tested using two different intramolecular hydroamination reactions.

Introduction

Homogeneous organometallic catalysts can readily be modified to fit the requirements of a wide variety of organic transformations. However, their recovery at the end of the reaction can be complex.[1] Therefore, active catalysts that feature the benefits of homogeneous catalysts and combine that with recyclability, and ease of use, are highly sought after. One strategy for accessing such catalysts is to graft homogeneous organometallic catalysts to insoluble solids (Figure 1).[2] This combination results in hybrid catalysts that utilize the benefits of homogeneous catalysts (defined structure and reactivity, tunability, and mechanistic information) and heterogeneous catalysts (simple reaction set-up, separation of products from the catalyst, and recyclability). Several different supports have been reported for such endeavour, including carbon-, silica-, alumina- and polymer-based materials.[3] While each surface can provide their own benefits, a key requirement for a viable solid-bound catalyst is a strong connection between the surface and the metal complex. This strong link is essential to avoid any leaching of the catalyst from the surface to the reaction media – a particularly important requirement for pharmaceutical reactions for example, where strict rules apply to any residual metal in the products. For this purpose we are interested in utilizing carbon-based solids as the insoluble support material, allowing us to connect the catalyst to the surface through strong covalent carbon-carbon bonds.

A variety of carbon materials, such as carbon black, graphene, and diamonds have been successfully used as catalyst support.[4] This work concentrates on carbon nanotubes

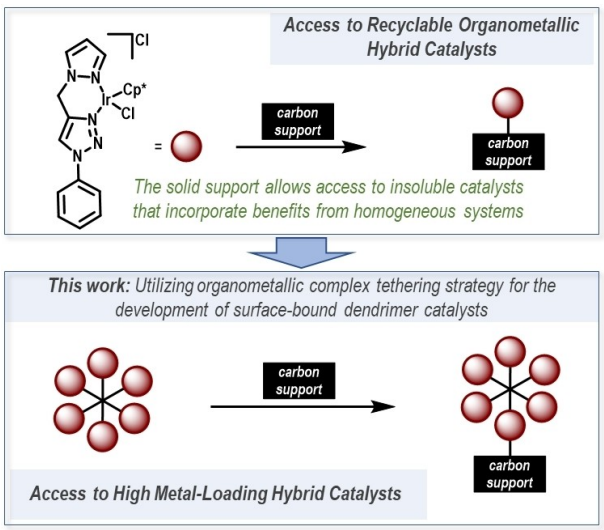

Figure 1. Top: Strategy for synthesizing surface bound well-defined organometallic complexes to enhance their recyclability. Bottom: Strategy for improving metal loading on surfaces by using dendrimeric catalysts.

[a] *Dr. I. Pernik[+]*
School of Chemistry, The University of Sydney,
Sydney, NSW 2006, Australia
E-mail: indrek.pernik@sydney.edu.au
https://www.sydney.edu.au/science/about/our-people/academic-staff/indrek-pernik.html
[b] *Dr. I. Pernik,[+] Prof. B. A. Messerle*
Department of Molecular Sciences, Macquarie University,
Sydney, NSW 2109, Australia
[c] *Dr. A. Desmecht,[+] Prof. S. Hermans, Prof. O. Riant*
Institute of Condensed Matter and Nanosciences, Molecules, Solids and Reactivity (IMCN/MOST) UCLouvain
Place Louis Pasteur 1, 1348 Louvain-la-Neuve, Belgium
E-mail: sophie.hermans@uclouvain.be
olivier.riant@uclouvain.be
https://uclouvain.be/fr/node/15912
https://uclouvain.be/fr/node/15931
[d] *Prof. B. A. Messerle*
School of Chemistry, The University of New South Wales,
Sydney, NSW 2052, Australia
[+] *These authors contributed equally to this work.*

Supporting information for this article is available on the WWW under https://doi.org/10.1002/ejic.202100380

Part of the "Supported Catalysts" Special Collection.

which provide a specialized form of graphene as a support.[5] Carbon nanotubes (single-/multi-walled NTs) have high physical and chemical stabilities, exceptional thermal and electrical conductivities, and relatively high surface areas (theoretical surface area of 1315 $m^2 g^{-1}$ for single walled NTs).[6] In addition, several synthetic approaches have been developed to transform NTs into chemical platforms for further post-functionalization reactions, providing a versatile set-up, suitable for grafting catalysts with different stabilities and requirements to the surface.

The grafting of transition metal complexes to carbon surfaces have resulted in successful catalysts with excellent recyclability, thus making transition metal complexes significantly more attractive for use in large scale applications.[4a,7] However, a limitation arising from the metal-to-surface ratio remains. On grafting metal complexes to carbon surfaces, low wt% of the bound metal is commonly observed (< 2 wt% Ir for C–C linkers, 5–12.5 wt% Ir for C–O linkers, see Table S2 in Supporting Information).[8] This is problematic, because to achieve sufficient loading of the metal complex in a catalytic mixture, relatively large amounts of the hybrid material will have to be present in the reaction media – a particularly relevant issue for large scale reactions.

One way to increase the relative amount of metal on the support is to utilize linkers that can bear more than one catalytically active metal centre within their structure. Such a requirement can readily be achieved using dendrimers. Dendrimers are well-defined hyper-branched macromolecules composed of monomeric units branching out from the central core. Despite the relatively complicated structures of the dendrimers, their synthesis is highly reproducible.[9] This has made dendrimers useful as encapsulating vectors in the field of drug delivery systems.[10] In addition, an established monometallic catalyst motif can readily be incorporated into the structure of a dendrimer by connection with its scaffold.[11] In doing so, the dendrimer hybrid catalyst obtained can retain the properties of the parent catalyst. These dendrimer catalysts have also displayed an increase in catalytic activity when compared to their monomeric analogues, termed the "dendritic effect".[12] This concept is analogous to the bimetallic effect, where a compound with two metal centres in close proximity can lead to improved catalytic activity compared to the monometallic systems.[8c,13]

Our groups have been involved in designing grafting methods of organic fragments on nanocarbons, as well as investigating the applications of supported catalysts.[4a,8b,14] Recently, we reported a straightforward and easy method for grafting dendrimers onto the surface of carbon nanotubes, which also allowed for the direct transformation of the dendrimers' terminal groups.[15] This led us to envisage an application of this methodology to the grafting of transition metal catalysts because of the potential advantage of increased metal loading and evaluating their efficiency through a well understood benchwork reaction. Alternative grafting methods developed in our groups will also be considered for comparison purposes.

Results and discussion

Synthesis

The ligand motif chosen for the dendrimers and the associated organometallic complexes was a pyrazole-triazole based ligand 4-((1H-pyrazol-1-yl)methyl)-1-phenyl-1H-1,2,3-triazole. This ligand motif provided an established route to organometallic complexes, as reported by Messerle previously.[16]

Overall, five different surface-bound species were synthesized: **3a**–**3d** (Scheme 1) and **3d'** (Scheme 2). The dendrimeric system **3a** was synthesized utilizing a method reported by Desmecht *et al.* where the CNT surface was lithiated using n-butyl lithium, followed by the addition of propargyl bromide to form the intermediate **1ab**.[15a,17] This intermediate (**1ab**) was then used for the grafting of a polyamidoamine (PAMAM) third generation dendrimer. The amino terminations of the commercially available third generation PAMAM dendrimer were first converted into azides after reaction with imidazole-1-sulfonyl azide sulfuric acid salt and copper sulfate. This intermediate species was directly reacted with the functionalized NT **1ab** using a Cu(I) catalyst. Then, click chemistry was further utilized to react the azido moieties of the azido-functionalized PAMAM-CNT hybrid with 1-(prop-2-yn-1-yl)-1*H*-pyrazole to yield **2a**. For the formation of the active catalyst, the $[Ir(Cp^*)Cl_2]_2$ (Cp* - pentamethylcyclopentadienyl) precursor was added to **2a**, leading to the formation of **3a**.

The starting precursor **1ab** was also used to synthesize a complex with a single metal centre as a comparison catalyst. For this, via the Sonogashira coupling reaction, compound **2b** was obtained with a pyrazole-triazole ligand attached to the CNT surface through a triple-bond linker. Similarly to **3a**, the desired iridium complex **3b** was obtained by addition of $[Ir(Cp^*)Cl_2]_2$ to the ligated surface precursor **2b**. To establish whether the link between the metal complex and the surface could play a role in the activity of the surface bound catalyst,[18] a direct CNT-C_6H_4-linked hybrid catalyst was also synthesized. For this, the initial lithiation of the CNT surface was followed by the addition of iPrOBPin (BPin = 4,4,5,5-tetramethyl-1,3,2-dioxaborolane) yielding **1c**.[19] This approach allowed for the synthesis of **2c** through Suzuki coupling, and as established for **3a** and **3b**, the addition of $[Ir(Cp^*)Cl_2]_2$ led to the formation of the desired metallo-species **3c**.

To avoid the n-butyl group on being attached to the surface, as a result of the initial surface lithiation step (*cf.* **3a**, **3b** and **3c**), another hybrid catalyst was designed. While the butyl group was expected to play a negligible role in the catalytic abilities of a large dendrimer unit attached to the CNT-surface, for a smaller organometallic complex, it could have a deleterious effect by reducing the substrates' access to the surface supported metal centre. To synthesize such a species a new approach in which B_2Pin_2 was reacted with lithium *tert*-butoxide to form an anionic intermediate which in turn could react with the nanotube surface through a metal-free diboration mechanism was exploited.[20] After this first step, a CNT-borate species without the butyl group attached was obtained (**1d**). As for **2c**, the ligated species **2d** was obtained through Suzuki coupling,

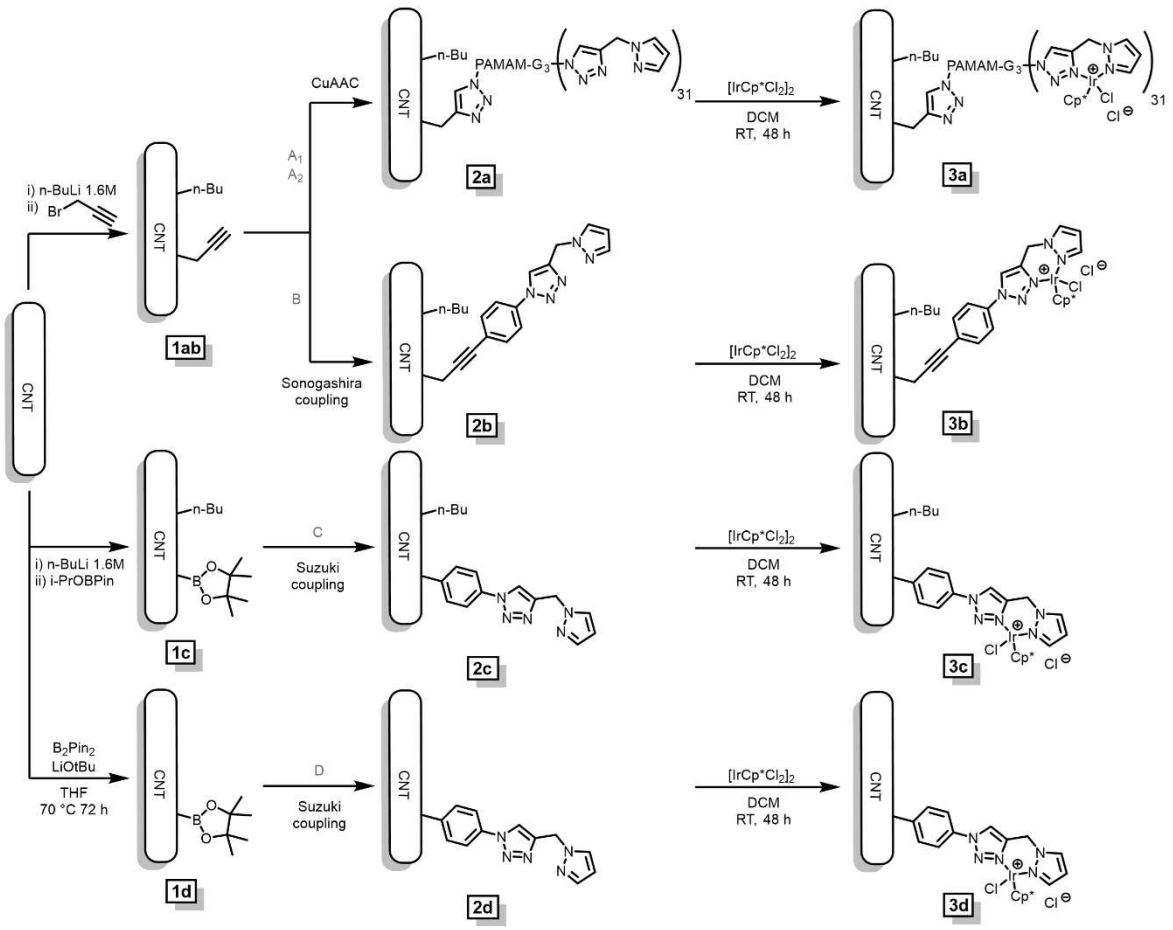

Scheme 1. The synthetic routes to the dendrimer-based catalyst **3 a** and the monometallic analogues (**3 b**–**3 d**). **A_1**) *i.* imidazole-1-sulfonyl azide.H_2SO_4, K_2CO_3, $CuSO_4.5H_2O$, PAMAM-$G_{3.0}$, MeOH, ON, RT. *ii.* **1 ab**, sodium ascorbate, 4 h, RT. **A_2**) N-propargylpyrazole, CuI, PMDETA, DMF, 72 h, RT. **B**) 4-((1H-pyrazol-1-yl) methyl)-1-(4-bromophenyl)-1H-1,2,3-triazole, CuI, $Pd(PPh_3)_4$, Et_3N, DMF, 72 h, 80 °C. **C**) 4-((1H-pyrazol-1-yl)methyl)-1-(4-bromophenyl)-1H-1,2,3-triazole, $Pd(PPh_3)_4$, K_2CO_3, DMF, 48 h, 80 °C. **D**) 4-((1H-pyrazol-1-yl)methyl)-1-(4-bromophenyl)-1H-1,2,3-triazole, $Pd(PPh_3)_4$, K_2CO_3, DMF, 72 h, 80 °C.

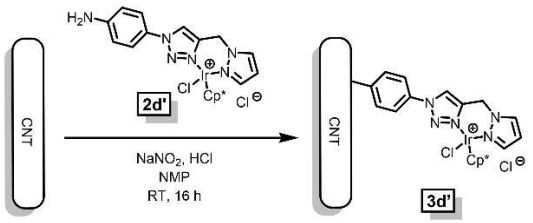

Scheme 2. Synthesis of the monometallic surface bound complex **3 d'** using the "grafted to" approach.

and the desired organometallic species **3 d** was accessed via the addition of $[Ir(Cp^*)Cl_2]_2$ to **2 d**.

The four hybrid catalysts (**3 a**–**3 d**) were synthesized using the "grafting from" approach, where the desired species were built on the surface step-by-step. The disadvantage of this strategy is that after a series of reactions, different entities are possibly present on the surface - due to the yields of each step being $<100\,\%$. However, the approach of adding the metal centre at the latest step possible avoids any potential changes to the metal centre arising from post-functionalization reactions.[18] To evaluate the synthetic approach, the hybrid material **3d'** was also synthesized via the "grafting to" approach, where a preformed iridium(III) complex **2d'** was directly attached to the carbon surface by reduction of aryl diazonium species onto the carbon surface (Scheme 2). This "grafting to" route has been reported for attaching a range of different organic and organometallic species to different carbon surfaces.[8c,21]

Characterization

The functionalization of the carbon nanotubes **1 ab**–**d** was confirmed by Thermogravimetric analysis (TGA), in agreement with previously reported results (Figure 2).[17,19] Two distinct weight losses were observed. The first between 250 and 700 °C, and then after 750 °C under inert atmosphere. The first loss is due to the decomposition of the surface groups grafted during functionalization and the second is linked to the decomposition of carbon nanotubes themselves.[17] The loading in propargylic and butyl groups of **1 ab** was evaluated at 4.0 wt%, whereas the

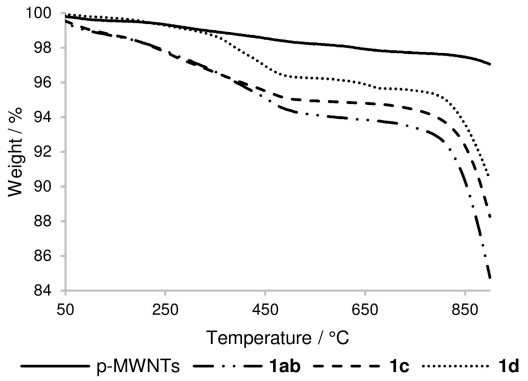

Figure 2. Comparative thermograms recorded under N_2 atmosphere for the first step of materials synthesis.

BPin and butyl groups (**1 c**), or solely BPin moieties (**1 d**), were determined to be 3.0 and 3.6 wt%, respectively. From this value, the carbon to functions ratio (C/R) were found to be: 97, 247 and 283, respectively (see Supporting Information for details on calculations).

The new materials obtained (intermediates **1 c** and **1 d**, immobilized ligands (**2 a**–**2 d**) and iridium complexes (**3 a**–**3 d'**)) were characterized by X-Ray Photoelectron Spectroscopy (XPS) and Inductively Coupled Plasma Atomic Emission Spectroscopy (ICP-AES) (Table 1 and Supporting Information), and the obtained data matches well with our previously reported results.[8c,18] Unfortunately, the boron content for the intermediate species **1 c** and **1 d** could not be quantified with XPS as it was below the detection limit of the instrument. However, Time-of-Flight Secondary Ion Mass Spectrometry (ToF-SIMS) and Thermogravimetric Analysis/Mass Spectrometry (TGA-MS) analyses, as described in a recent report, confirmed their presence.[19] Regarding the synthesis of **2 a**, the successful transformation of dendrimer azido terminations into triazole groups was confirmed via the disappearance of the peak component at 405 eV in the N1s region that is associated with the electron-poor nitrogen of the azido groups (Supporting Information, Figure S1).[22]

The surface iridium content ranges from 0.02 at% to 0.08 at % for the monometallic organometallic hybrid complexes **3 b**–**3 d'** (XPS data), with the corresponding wt% values ranging from 0.3–1.2 (ICP-AES). The highest iridium loading was, as expected, obtained for **3 a** with 0.82 at.% and 8.3 wt% as the multiple terminations of the dendrimer allow the formation a higher number of organometallic complexes.

The route for synthesizing the monometallic CNT-bound system **3 d** presents a valuable strategy for accessing CNT-bound organometallic complexes. Interestingly, the alternative "grafted to" route via diazonium salts (*cf.* Scheme 2), which has been successful for carbon black, reduced graphene oxide and glassy carbon surfaces, has not been effective for accessing CNT-bound species previously, and within this work led to substantially lower iridium content on the surface (*i.e.* **3 d** *vs* **3 d'**).[4a,8c,14a,18] However, a potentially feasible slightly modified route that utilizes diazonium salts has recently been reported by Metwally *et al.*[23]

XPS spectral data for the Ir 4f narrow scans for **3 a**–**3 d'** were all effectively identical to each other, indicative of similar iridium environments when comparing single-site and dendrimeric organometallic catalysts (Supporting Information, Figure S2). The analogous Ir 4f XPS spectra is an important fact for the catalysis study, allowing for a more straightforward comparison.

XPS data also provided additional information about the structure of the dendrimeric system. Although **3 a** is depicted as attached with one termination to the surface for the sake of clarity, it would be idealistic to consider it as such. The degree of functionalized PAMAM terminations was evaluated by comparing the XPS N/Ir ratio with the ones calculated for each increment of functionalization, from 1 to 31. The experimental atomic ratio N/Ir of 10.0 corresponds to a dendrimeric structure, with 23 out of 31 terminations converted into organometallic complexes. This assumption requires that the XPS analysis reflects the dendrimer in its whole (3.1 nm diameter) and is not limited by the depth of analysis (~5 nm).[24]

Catalysis

For achieving optimum catalytic outcomes, the substantially higher wt% of iridium on the dendrimeric catalyst surface (>6.9 times higher iridium loading for **3 a** compared to **3 d**, with the corresponding values of 7.5, 11.8 and 27.7 when compared to **3 b**, **3 c** and **3 d'**, respectively) was encouraging. The higher

Table 1. XPS and ICP-AES characterization of immobilized ligands (**2 a**–**2 d**) and iridium complexes (**3 a**–**3 d'**).

	C_{1s}	O_{1s}	N_{1s}		Cl_{2p}			Ir_{4f}	
	[at.%]	[at.%]	[at.%]	[eV]	[at.%]	[ev]	[at%][a]	[eV]	[wt%][b]
2 a	83.39	6.87	9.49	400.1	–	–	–	–	–
3 a	82.62	6.63	8.22	400.4	1.71	198.7	0.82	62.6	8.3
2 b	96.18	2.67	0.79	400.7	–	–	–	–	–
3 b	96.52	2.66	0.56	400.1	0.19	199.8	0.07	62.7	1.1
2 c	98.55	1.17	0.28	401.6	–	–	–	–	–
3 c	98.48	1.10	0.26	400.8	0.12	199.9	0.04	62.7	0.7
2 d	97.01	2.50	0.49	401.1	–	–	–	–	–
3 d	97.30	1.81	0.68	401.2	0.15	198.5	0.08	62.9	1.2
3d'	98.83	0.88	0.21	400.6	0.06	199.0	0.02	62.4	0.3

[a] Determined by XPS. [b] Determined by ICP-AES.

relative amount of iridium on the CNT surface could be beneficial in the development of a new generation of insoluble surface bound catalysts, as the relative amount of inactive solid material is substantially lower. In terms of practically handling the new catalysts, the higher relative ratio of iridium to solid allows for the weighing of much less catalyst into the reaction mixtures, potentially providing a route to utilizing organometallic complexes more efficiently in large industrial settings. In fact, the iridium loading of the "grafting to" species **3 d'** was found to be too low for any reliable catalytic data to be obtained due to the large amount of solid material in the reaction mixture impeding the stirring process.

To investigate the catalytic abilities of the hybrid catalysts **3 a**–**3 d**, a simple hydroamination reaction was chosen: the intramolecular hydroamination of 1-pentynamine (Scheme 3).[25] This simple reaction with limited scope for side reactions is well set to investigate the effects that might arise from the different materials. In addition, as substrate **A** is sterically low demanding, the inherently bulky structure of the dendrimer **3 a** was not expected to lead to large effects. Similarly, the closeness of the surface to the metal centres in the organometallic catalysts (**3 b**–**3 d**) should also have limited effect on the efficiency of the catalysis. Further, it has been previously shown that the pyrazole triazole based iridium(III) complexes with Cp* and chlorido co-ligands are active catalysts in this hydroamination transformation.[8c]

In all cases the amount of catalyst used was kept at 1 mol% iridium loading. The basis for the iridium content was taken from ICP-AES data to exclude any errors arising from XPS depth of analysis considerations. The catalytic runs were carried out in 1.0 mL of toluene solvent, 0.06 mmol of 1-pentynamine (**A**) at 100 °C allowing for a viable timeframe for comparisons. The reactions were followed by ^{1}H NMR spectroscopy and in all cases the reactions led to clean conversion of 1-pentynamine (**A**) to 5-methyl-3,4-dihydro-2H-pyrrole (**B**) (Scheme 3), matching well with the previously reported data.[25] When comparing the catalysts' activity, relatively small changes were seen for the

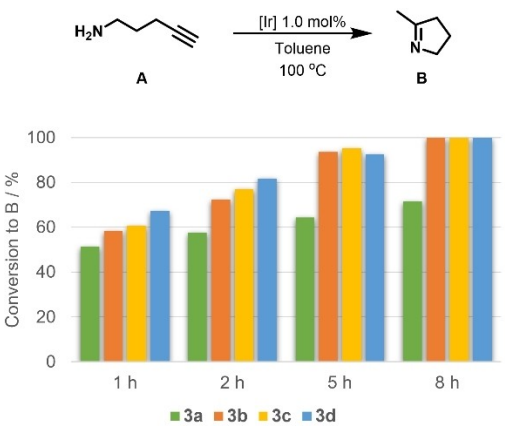

Scheme 3. Hydroamination transformation of **A** to **B** using **3 a**–**3 d** as catalysts. Catalysis conditions: 1.0 mol% [Ir] loading, 0.06 mmol **A**, 1.0 mL toluene, 100 °C. The reactions were conducted in sealed vials and were followed using ^{1}H NMR spectroscopy.

monometallic species **3 b**–**3 d** with conversions to **B** of 58–67% observed after one hour of stirring, and >90% conversion seen at the 5-hour mark. After 8 hours, all three catalysts (**3 b**–**3 d**) demonstrated >98% conversion to the desired product **B**. Interestingly, substantially different results were observed for the dendrimeric catalyst **3 a**. While at the 1-hour point, conversion comparable to the monometallic systems was obtained (>50%), after 5 hours still only 63%, and when left to stir for 8 hours less than 70% of **A** had been converted to **B**.

Based on the conversions all three simple organometallic systems (**3 b**–**3 d**) could be considered as the more successful catalysts with insignificant differences arising from the different linkers. However, some practical aspects should be considered. By far the easiest catalyst to use was the dendrimeric system **3 a**. The significantly higher iridium loading on the surface meant that a fraction of the catalyst had to be weighed into the mixture. This smaller amount of solid in the mixture (1.4 mg mL^{-1} (**3 a**) *vs* 9.1 mg mL^{-1} (**3 d**)) also resulted in substantially easier stirring, and more reliable results, as the catalyst remained in the reaction solution (as outlined in Supporting Information). In the case of **3 b** (10.8 mg mL^{-1}) and **3 d**, the stirring was reliable, however, it was noted that occasionally the solid catalyst was being pushed to the walls of the vial above the solvent level. For **3 c** (17.0 mg mL^{-1}), occasional issues with stirring were also observed. At such low volumes, these issues could be overcome by occasionally shaking the reaction mixture, but in large scale catalytic transformations, the use of low metal loading hybrid catalysts would be substantially more challenging than the use of high metal loading hybrid catalysts.

While in practical terms, the dendrimeric catalyst **3 a** was the easiest to use, its catalytic activity was not comparable to the monometallic catalysts. To test whether the reaction using the dendrimer **3 a** as a catalyst would benefit from longer reaction times the catalysis was allowed to proceed for 24 hours. Interestingly, even at such prolonged reaction time, only 89.1% conversion to **B** was observed. This reduction in catalysis rate over time indicates that a catalyst deactivation occurs. This was unexpected, as the dendrimeric (**3 a**) and the monometallic (**3 d**) catalysts' iridium centres should be identical thus similar decomposition pathways would be expected. To investigate whether the formed product might be inhibiting the dendrimeric catalyst, recycling reactions were performed using **3 a** and **3 d**. For this, the reaction mixture was washed at the end of the reaction (8 hours) with 3×4 mL of toluene, and centrifuged. The vial was then recharged with **A** (0.06 mmol) and toluene (1 mL). For the monometallic catalyst **3 d**, this resulted in slightly reduced catalysis rate (87.5% conversion to **B** after 5 h, >98% after 8 h). The dendrimeric catalyst (**3 a**) was effectively inactive after the wash, with only 13.9% conversion seen after 5 hours (*cf.* 63.5% after 5 hours in the first run for **3 d**). Both **3 a** and **3 d** lost some catalytic activity, however this deactivation seems to affect the dendrimeric system more. No improvements were observed when the reaction was prepared and conducted under argon or at a lower temperature (<70 °C).

The access to the pyrazole triazole iridium complex on the CNT-surface allowed us to directly compare the CNT-bound catalyst to other surfaces with the same iridium complex

attached. For this comparison, an additional set of hydroamination transformations were conducted for the cyclization of 6-(2-aminophenyl)hex-5-yn-1-ol (**C**) to 4-(1H-indol2-yl)butan-1-ol (**D**) (Scheme 4). Binding *et al.* have demonstrated that iridium pyrazole-triazole catalysts attached to carbon black (CB) and reduced graphene oxide (rGO) surfaces act as catalysts for this transformation.[8c] For simplicity, this comparison study was limited to catalysts **3 a** and **3 d**.

For the hydroamination transformation of **C** to **D**, the monometallic complex **3 d** outperformed the catalysis results reported for the analogous CB- or rGO-bound catalysts under the same reaction conditions (Figure 3). After one hour, 27% conversion to **D** was seen for **3 d** (*cf.* 18% for CB-bound, and 27% for rGO-bound), and after 5 hours 79.7% conversion was obtained (*cf.* 47% for CB-bound, and 61% for rGO-bound). This comparison demonstrates that CNT surfaces are at least as good as CB and rGO surfaces for hydroamination transformation. At the same time, the dendrimeric catalyst **3 a** showed low conversions, with just 11.5% conversion to **D** seen after 5 hours (17.8% after 8 hours). This comparison of two catalytic transformations (**A** to **B** *vs* **C** to **D**) provides us a potential clue about the reactivity of the dendrimer. As postulated, the inherently larger structure of the dendrimer might be the reason for slower activity. By changing the substrate from a small amine (**A**) to a much larger (**C**) a significant loss in reactivity was seen for the dendrimeric **3 a**, compared to the monometallic **3 d**.

Overall, this preliminary set of catalytic results demonstrated that there are strong practical arguments for utilizing surface-bound dendrimers as catalysts compared to the simpler surface-bound monometallic complexes. However, there are clearly deactivation pathways that can affect dendrimeric systems more readily than the monometallic catalysts. The results are encouraging for further exploration into the reactivity of dendrimers as catalysts with and without attached solid supports using a wider range of catalytic transformations and reaction conditions, to pinpoint the reasons behind their different behaviour when compared to simple organometallic complexes.

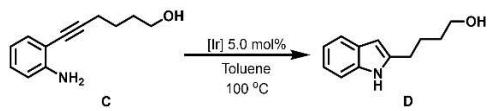

Scheme 4. Hydroamination transformation of **C** to **D**. Catalysis conditions: 5.0 mol% [Ir] loading, 0.06 mmol **C**, 1.0 mL toluene, 100 °C. The reactions were conducted in sealed vials and were followed using ^{1}H NMR spectroscopy.

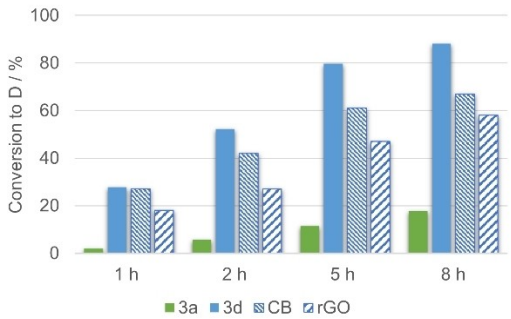

Figure 3. Hydroamination transformation of **C** to **D** using **3 a** and **3 d** as catalysts. CB and rGO correspond to reported catalysis data of iridium(III) pyrazole-triazole complexes on carbon black and reduced graphene oxide surfaces, respectively.[8c]

Conclusions

Within this work five carbon surface bound pyrazole-triazole iridium complexes were synthesized and analytically characterized. One of the catalysts contained a dendrimer linker (**3 a**), while the other four were monometallic organometallic complexes bound to the surface (**3 b**–**3 d'**). The analytical data indicated that all five catalysts contained analogous iridium centres, but the use of a dendrimeric system led to a significantly higher (>6.9 times) iridium content on the surface, allowing for practical benefits in the catalysis set-up.

The intramolecular hydroamination catalysis results demonstrated that monometallic complexes **3 b**–**3 d** are efficient catalysts for the hydroamination reaction of 1-pentynamine, while the dendrimeric catalyst **3 a** showed good initial activity but limited reactivity in the latter stages of the catalytic reaction. Carbon nanotube bound catalysts **3 a** and **3 d** were also compared to previously reported carbon black and reduced graphene oxide bound analogous systems for the hydroamination reaction of 6-(2-aminophenyl)hex-5-yn-1-ol, indicating the excellent suitability of MWNTs as surfaces supports for organometallic catalysts.

The next target within this work is to establish a better understanding behind reasons for the different catalytic activity of the dendrimeric systems, when compared to the monometallic analogues.

Experimental section

All reactions were performed under argon or nitrogen atmosphere using Schlenk glassware. Commercial reagents were used as received while solvents were distilled on Na before use and stored under nitrogen on molecular sieve. MWNTs were obtained from Nanocyl (Belgium) (NC 7000 Thin MWNTs, 95+% C purity) and were used without further purification.

The catalysis substrates 1-pentynamine (**A**) and 6-(2'-aminophenyl) hex-5-yn-1-ol (**C**) were synthesised based on previously reported procedures.[26] The substrate **A** was vacuum distilled at −10 °C to remove the remaining diethyl ether.

X-ray photoelectron spectroscopy. XPS analyses were carried out at room temperature with a SSIX-probe (SSX 100/206) photoelectron spectrometer from Surface Science Instruments (USA) equipped with a monochromatized microfocus Al X ray source. Samples were stuck onto small sample holders with double-face adhesive tape and then placed on an insulating home-made ceramic carousel (Macor®, Switzerland). Charge effects were avoided by placing a nickel grid above the samples and using a flood gun set at 8 eV. The binding energies were calculated with respect to the *C*-(C,C) component of the C_{1s} peak fixed at 284.4 eV. Data treatment was

performed with the CasaXPS program (Casa Software Ltd., UK). The peaks were decomposed into a sum of Gaussian/Lorentzian (85/15) after subtraction of a Shirley type baseline.

Thermogravimetric analysis. Thermograms were recorded on a TGA/SDTA 851[e] simultaneous DSC-TGA instrument from METTLER TOLEDO. These analyses were carried out with a heating ramp of 10 °C/min and under N_2 flow (105 ml/min) with the samples (3–5 mg) placed into alumina containers.

Nuclear magnetic resonance. NMR spectra were recorded on BRUKER spectrometers (300, 400 and 500 MHz for ^{1}H, 75 MHz for ^{13}C). Chemical shifts are reported in d ppm from tetramethylsilane with the solvent resonance as the internal standard for ^{1}H NMR.

Mass spectrometry. HRMS were recorded on a Q-Extractive orbitrap from ThermoFisher. Samples were ionized by APCI (capillary temperature: 250 °C, vaporizer temperature: 250 °C, sheath gas flow rate: 20).

(Bulk) Elemental Analysis. Single-run bulk elemental analyses (ICP-AES for metal and microgravimetry for CHN) were performed by the independent company Medac Ltd. in the UK.

Synthesis

Procedure for the synthesis of 4-((1H-pyrazol-1-yl) methyl)-1-(4-bromophenyl)-1H-1,2,3-triazole ligand

A mixture of pyrazole (2 g, 29.4 mmol, 1 eq), K_2CO_3 (20 g, 147.3 mmol, 5 eq.) and propargyl bromide (80 wt% solution in toluene, 7 mL, 47 mmol, 1.6 eq.) in 50 mL acetone is refluxed for 16 h in a round-bottom flask equipped with a condenser. The reaction mixture is then cooled down to RT, filtered and the solvent is removed under reduced pressure. The crude product is purified by column chromatography on silica gel (cyclohexane:AcOEt 3:1) to yield 1-(prop-2-yn-1-yl)-1*H*-pyrazole as a clear oil (34% yield). **^{1}H NMR** (300 MHz, $CDCl_3$) δ 7.60 (d, J = 2.3 Hz, 1H), 7.54 (d, J = 1.5 Hz, 1H), 6.30 (t, J = 2.1 Hz, 1H), 4.95 (d, J = 2.6 Hz, 2H), 2.50 (t, J = 2.6 Hz, 1H).

A solution of 4-bromoaniline (3.4 g, 20 mmol, 1 eq.) in 20 mL HCl 6 M in a round-bottom flask is cooled down at 0 °C. A solution of $NaNO_2$ (2.07 g, 30 mmol, 1.5 eq.) in 50 mL H_2O is added dropwise and the reaction mixture is stirred 30 min at 0 °C. A solution of NaN_3 (5.2 g, 80 mmol, 4 eq.) in 50 mL H_2O is added dropwise and the reaction mixture is stirred 3 h at RT. Then, the aqueous phase is extracted twice with AcOEt, the organic layers are washed with H_2O, dried over Na_2SO_4, filtered and evaporated under reduced pressure to give 1-azido-4-bromobenzene as a brown oil (86%). **^{1}H NMR** (300 MHz, $CDCl_3$) δ 7.50–7.42 (m, 2H), 6.95–6.86 (m, 2H).

In a Schlenk flask under inert atmosphere 424 mg 1-(prop-2-yn-1-yl)-1*H*-pyrazole (4 mmol, 1 eq.) are added together with 792 mg 1-azido-4-bromobenzene (4 mmol, 1 eq.), 76 mg CuI (0.4 mmol, 10 mol.%) and 84 μL PMDETA (0.4 mmol, 10 mol.%). A green precipitate is formed after 5 minutes and the reaction mixture is stirred for 4 h at RT. The solvent is removed under reduced pressure and the green residue is taken up in DCM. The organic phase is washed with H_2O and five times with a 10 wt% EDTA solution until the aqueous layer is colorless. The organic phase is dried over Na_2SO_4, filtered and evaporated under reduced pressure to give 4-((1*H*-pyrazol-1-yl)methyl)-1-(4-bromophenyl)-1*H*-1,2,3-triazole as yellow brownish solid (72%). **^{1}H NMR** (300 MHz, DMSO) δ 8.82 (s, 1H), 7.94–7.71 (m, 5H), 7.46 (d, J = 1.4 Hz, 1H), 6.27 (t, J = 2.0 Hz, 1H), 5.49 (s, 2H). **^{13}C NMR** (75 MHz, DMSO) δ 144.67, 139.50, 136.18, 133.23, 130.45, 122.63, 122.48, 121.83, 106.04, 46.69. **HRMS (APCI)** calculated for $C_{12}H_{11}N_5{}^{79}Br$ $[M+H]^+$ 304.01923, found 304.01921.

Procedure for the syntheses of 4-(4-((1H-pyrazol-1-yl) methyl)-1H-1,2,3-triazol-1-yl)aniline and corresponding Iridium organometallic complex

A solution of 4-nitroaniline (2.76 g, 20 mmol, 1 eq.) in 20 mL HCl 6 M in a round-bottom flask is cooled down at 0 °C. A solution of $NaNO_2$ (2.07 g, 30 mmol, 1.5 eq.) in 50 mL H_2O is added dropwise and the reaction mixture is stirred 30 min at 0 °C. A solution of NaN_3 (5.2 g, 80 mmol, 4 eq.) in 50 mL H_2O is added dropwise and the reaction mixture is stirred 3 h at RT. Then, the aqueous phase is extracted twice with AcOEt, the organic layers are washed with H_2O, dried over Na_2SO_4, filtered and evaporated under reduced pressure to give 1-azido-4-nitrobenzene as a brown oil (86%). **^{1}H NMR** (300 MHz, $CDCl_3$) δ 7.50–7.42 (m, 2H), 6.95–6.86 (m, 2H).

In a Schlenk flask under inert atmosphere 424 mg 1-(prop-2-yn-1-yl)-1*H*-pyrazole (4 mmol, 1 eq.) are added with 656 mg 1-azido-4-nitrobenzene (4 mmol, 1 eq.), 76 mg CuI (0.4 mmol, 10 mol.%) and 84 μL PMDETA (0.4 mmol, 10 mol.%). The reaction mixture is stirred for 4 h at RT. The solvent is removed under reduced pressure and the green residue is taken up in DCM. The organic phase is washed with H_2O and thrice with a 10 wt% EDTA solution until the aqueous layer is colorless. The organic phase is dried over Na_2SO_4, filtered and evaporated under reduced pressure. The crude solid is washed with Et_2O to give 4-((1*H*-pyrazol-1-yl)methyl)-1-(4-nitrophenyl)-1*H*-1,2,3-triazole as yellow brownish solid (56%). **^{1}H NMR** (300 MHz, DMSO) δ 9.01 (s, 1H), 8.50–8.39 (m, 2H), 8.29–8.15 (m, 2H), 7.86 (d, J = 2.2 Hz, 1H), 7.47 (dd, J = 1.8, 0.4 Hz, 1H), 6.28 (t, J = 2.1 Hz, 1H), 5.53 (s, 2H).

A suspension of 4-((1*H*-pyrazol-1-yl)methyl)-1-(4-nitrophenyl)-1*H*-1,2,3-triazole (2 mmol, 1 eq.), Pd on carbon (10 wt% in Pd, 212 mg, 0.2 mmol, 10 mol.%) in 30 mL is introduced in a round-bottom flask equipped with a condenser. Hydrazine (5 mL, 100 mmol, 50 eq.) is added and the suspension is stirred for 16 h at 45 °C. Then, the reaction mixture is filtered over a pad of celite and the filtrate is evaporated under reduced pressure to give 4-(4-((1*H*-pyrazol-1-yl) methyl)-1*H*-1,2,3-triazol-1-yl)aniline as a yellow solid (96%). **^{1}H NMR** (300 MHz, $CDCl_3$) δ 7.78 (s, 1H), 7.55 (dd, J = 8.1, 2.0 Hz, 2H), 7.43–7.34 (m, 2H), 6.75–6.65 (m, 2H), 6.27 (t, J = 2.1 Hz, 1H), 5.50 (s, 2H), 3.92 (bs, 2H).

To a solution of 4-(4-((1H-pyrazol-1-yl)methyl)-1H-1,2,3-triazol-1-yl) aniline (48 mg, 0.2 mmol, 1 eq.) in 5 mL MeOH is added $[IrCp^*Cl_2]_2$ (79.8 mg, 0.1 mmol, 0.5 eq.). The reaction mixture is stirred at RT until complete dissolution of $[IrCp^*Cl_2]_2$ (*ca.* 30 min.). The solvent is then removed under reduced pressure to yield the corresponding iridium organometallic complex **2e** as a yellow solid (quantitative). **^{1}H NMR** (300 MHz, $CDCl_3$) δ 9.02 (s, 1H), 8.37 (d, J = 2.3 Hz, 1H), 7.64 (d, J = 2.1 Hz, 1H), 7.41 (d, J = 8.8 Hz, 2H), 7.07 (d, J = 16.2 Hz, 1H), 6.81 (d, J = 8.7 Hz, 2H), 6.45 (t, J = 2.5 Hz, 1H), 5.09 (d, J = 16.0 Hz, 1H), 1.67 (s, 15H). **^{13}C NMR** (75 MHz, $CDCl_3$) δ 143.58, 140.03, 135.50, 127.02, 125.05, 123.62, 122.19, 115.63, 108.27, 88.74, 45.83, 9.19. **HRMS (ESI)** calculated for $C_{22}H_{27}N_6{}^{35}Cl^{191}Ir$ $[M-Cl]^+$ 601.15862, found 601.15901.

Procedure for the synthesis of propargyl-functionalized MWNTs 1ab

1 g of MWNTs and 625 mL of dry diethyl ether are introduced in a flame-dried Schlenk. The resulting suspension is sonicated for 30 min. The black suspension is then cooled down to −78 °C and 53 mL of 1.6 M *n*-BuLi solution in hexanes (85 mmol) are added. The reaction mixture is allowed to reach room temperature and is stirred for 16 hours. 19 mL of propargyl bromide solution (80 wt% in toluene, 170 mmol) are added and the suspension is stirred for another 4 hours. The reaction is quenched with 50 mL EtOH. 50 mL

of distilled water are added and acidic to neutral pH is obtained with 1 M HCl aqueous solution. The organic layer is washed thrice with water and then filtered on a PVDF Millipore membrane (0.22 μm). The black solid is washed with 1 L of THF and 1 L of EtOH. The resulting powder is finally dried under vacuum.

Procedure for the synthesis of PAMAM/MWNTs-supported ligand 2 a

A suspension is prepared by adding 95.0 mg of imidazole-1-sulfonyl azide.H_2SO_4 (0.351 mmol, 4.8 eq.), 79.5 mg K_2CO_3 (0.846 mmol, 11.5 eq.) and 3.1 mg of $CuSO_4.5H_2O$ (0.012 mmol, 16 mol%) in a 10 mL round-bottom flask, 5 mL of MeOH is then added and the mixture is stirred for 2 minutes to obtain a suspension. 0.38 ml of a 20 wt% commercial solution of PAMAM $G_{3.0}$ in MeOH (0.076 mmol, 1 eq.) is then added and the mixture is stirred overnight at room temperature. 240 mg of **1 ab** are suspended in 100 mL of MeOH in a round-bottom Schlenk flask by sonication during 60 minutes. The suspension containing the PAMAM-azide is then added by canula to the nanotube suspension under stirring. 4.8 mg of sodium ascorbate (0.024 mmol, 32 mol%) is added and the reaction flask is covered with aluminum foil to prevent contact with light. The suspension is stirred for 4 hours and then filtered under vacuum over a PVDF Millipore membrane (0.22 μm) and the obtained powder is washed successively with 300 mL THF, 300 mL MeOH, 100 mL concentrated aqueous NH_3, 100 mL EDTA 1 wt% (pH 8), 300 mL H_2O, 300 mL MeOH and 300 mL Et_2O. The obtained black powder is then dried under vacuum to yield immobilized PAMAM-$G_{3.0}$.

250 mg of PAMAM-$G_{3.0}$ immobilized on MWNTs are sonicated in 100 mL dry DMF in a Schlenk flask for 60 minutes. 62 mg CuI (0.325 mmol, 0.1 eq.), 68 μL of PMDETA (0.325 mmol, 0.1 eq.) and 344 mg 1-(prop-2-yn-1-yl)-1*H*-pyrazole (3.25 mmol, 1 eq.) are then added and the suspension is stirred for 72 hours. The stirring bar is removed and 50 mL of DMF are added. The reaction mixture is sonicated for 5 min and then filtered on a PTFE Millipore membrane (0.45 μm). The solid is washed with 400 mL MeOH and 400 mL DCM and then dispersed in 100 mL EtOH and sonicated for 60 min. The suspension is filtered on a PVDF Millipore membrane (0.45 μm) and the black powder is washed with 200 mL of 25 % ammonia solution, 100 mL of 1 wt% EDTA solution in water at pH 8, 400 mL of distilled water, 400 mL of MeOH and 400 mL of Et_2O. The resulting powder is finally dried under vacuum to give **2 a**.

Procedure for the synthesis of MWNTs-supported catalyst 3 a

240 mg of 2a are dispersed in 100 mL of CH_2Cl_2 and the suspension is sonicated for 60 min. 101 mg of $[IrCp^*Cl_2]_2$ (0.12 mmol) is added and the reaction mixture is stirred for 48 h at room temperature. The suspension is filtered on a PVDF Millipore membrane (0.45 μm). The black solid is washed with 400 mL of THF, 400 mL of EtOH and 400 mL of Et_2O. The resulting powder is finally dried under vacuum to give 3a.

Procedure for the synthesis of MWNTs-supported ligand 2 b

220 mg alkynyl-MWNT of **1 ab** are introduced in a flame-dried Schlenk with 100 mL of dry DMF under Ar. The suspension is sonicated for 60 min before the addition of CuI (41.6 mg, 0.22 mmol, 0.4 eq.), $Pd(PPh_3)_4$ (127 mg, 0.11 mmol, 0.2 eq.), Et_3N (3.1 mL, 22 mmol, 40 eq.) and 4-((1H-pyrazol-1-yl)methyl)-1-(4-bromophenyl)-1H-1,2,3-triazole (166.6 mg, 0.55 mmol, 1 eq.). The suspension is then stirred for 72 h at 80 ○C, cooled down to RT, 50 mL of DMF are then added and the mixture is sonicated for 5 min before filtration on a PTFE Millipore membrane (0.22 μm). The black solid is washed with successively 300 mL THF and 300 mL MeOH. The solid is taken up in 100 mL EtOH and sonicated for 1 h. Then the suspension is filtered on a PVDF Millipore membrane (0.45 μm) and washed with 200 mL concentrated aqueous NH_3, 100 mL EDTA 1 wt% aqueous solution (pH 8), 300 mL H_2O, 300 mL MeOH and 300 mL Et_2O. The obtained black powder is finally dried under vacuum to give **2 b**.

Procedure for the synthesis of MWNTs-supported catalyst 3 b

220 mg of **2 b** are dispersed in 100 mL of CH_2Cl_2 and the suspension is sonicated for 60 min. 33 mg of $[IrCp^*Cl_2]_2$ (0.04 mmol) is added and the reaction mixture is stirred for 48 h at room temperature. The suspension is filtered on a PVDF Millipore membrane (0.45 μm). The black solid is washed with 400 mL of THF, 400 mL of EtOH and 400 mL of Et_2O. The resulting powder is finally dried under vacuum to give **3 b**.

Procedure for the synthesis of BPin-functionalized MWNTs 1 c

120 mg of MWNTs and 75 mL of dry diethyl ether are introduced in a flame-dried Schlenk flask. The resulting suspension is sonicated for 60 min. The black suspension is then cooled down to −78 °C and 6.4 mL of 1.6 M *n*-BuLi solution in hexanes (10.24 mmol, 1 eq.) are added. The reaction mixture is allowed to reach room temperature and is stirred for 16 hours. 4.18 mL of 2-isopropoxy-4,4,5,5-tetramethyl-1,3,2-dioxaborolane i-PrOBPin (20.48 mmol, 2 eq.) are added and the suspension is stirred for another 4 hours. The reaction is quenched with 5 mL EtOH. 5 mL of distilled water are added and acidic to neutral pH is obtained with 1 M HCl aqueous solution. The suspension is filtered on a PVDF Millipore membrane (0.22 μm) and the black powder is taken up in 50 mL diethyl ether and sonicated for 5 min. The organic suspension is washed thrice with water and then filtered on a PVDF Millipore membrane (0.22 μm). The black solid is washed with 200 mL of THF and 200 mL of EtOH. The resulting powder is finally dried under vacuum.

Procedure for the synthesis of MWNTs-supported ligand 2 c

220 mg of **1 c** and 100 mL of DMF are added to a flame-dried Schlenk under inert atmosphere and sonicated for 60 min. 250 mg 4-((1H-pyrazol-1-yl)methyl)-1-(4-bromophenyl)-1H-1,2,3-triazole (0.83 mmol, 1 eq.), 230 mg of K_2CO_3 (1.66 mmol, 2 eq.) and 96 mg of $Pd(PPh_3)_4$ (0.83 mmol, 0.1 eq.) are added to the resulting suspension. The reaction mixture is heated at 80 °C for 48 hours and then cooled down to room temperature. Then, 50 mL of DMF are added and the mixture is sonicated for 5 min before filtration on a PTFE Millipore membrane (0.22 μm). The black solid is washed with successively 300 mL THF and 300 mL MeOH. The solid is taken up in 100 mL EtOH and sonicated for 1 h. Then the suspension is filtered on a PVDF Millipore membrane (0.45 μm) and washed with 200 mL concentrated aqueous NH_3, 100 mL EDTA 1 wt% aqueous solution (pH 8), 300 mL H_2O, 300 mL MeOH and 300 mL Et_2O. The obtained black powder is finally dried under vacuum to give **2 c**.

Procedure for the synthesis of MWNTs-supported catalyst 3 c

200 mg of **2 c** are dispersed in 100 mL of CH_2Cl_2 and the suspension is sonicated for 60 min. 30 mg of $[IrCp^*Cl_2]_2$ (0.036 mmol) is added and the reaction mixture is stirred for 48 h at room temperature. The suspension is filtered on a PVDF Millipore membrane (0.45 μm). The black solid is washed with 400 mL of THF, 400 mL of EtOH and

400 mL of Et_2O. The resulting powder is finally dried under vacuum to give **3 c.**

Procedure for the synthesis of BPin-functionalized MWNTs 1 d

In a flame-dried Schlenk under inert atmosphere, a suspension of 250 mg MWNTs in 125 mL dry THF is sonicated for 60 minutes. Then, 500 mg LiO*t*Bu (6.25 mmol, 2 eq.) and 792 mg B_2Pin_2 (3.12 mmol, 1 eq.) are introduced and the suspension is stirred for 72 h at 70 °C. The suspension is brought back to RT and filtered on a PVDF Millipore membrane (0.22 μm). The black solid is washed with successively 300 mL THF, 300 mL H_2O, 300 mL MeOH and 300 mL Et_2O. The obtained black powder was finally dried under vacuum.

Procedure for the synthesis of MWNTs-supported ligand 2 d

220 mg of **1 d** and 100 mL of DMF are added to a flame-dried Schlenk under inert atmosphere and sonicated for 60 min. 250 mg 4-((1H-pyrazol-1-yl)methyl)-1-(4-bromophenyl)-1H-1,2,3-triazole (0.83 mmol, 1 eq.), 230 mg of K_2CO_3 (1.66 mmol, 2 eq.) and 96 mg of $Pd(PPh_3)_4$ (0.83 mmol, 0.1 eq.) are added to the resulting suspension. The reaction mixture is heated at 80 °C for 48 hours and then cooled down to room temperature. Then, 50 mL of DMF are added and the mixture is sonicated for 5 min before filtration on a PTFE Millipore membrane (0.22 μm). The black solid is washed with successively 300 mL THF and 300 mL MeOH. The solid is taken up in 100 mL EtOH and sonicated for 1 h. Then the suspension is filtered on a PVDF Millipore membrane (0.45 μm) and washed with 200 mL concentrated aqueous NH_3, 100 mL EDTA 1 wt% aqueous solution (pH 8), 300 mL H_2O, 300 mL MeOH and 300 mL Et_2O. The obtained black powder is finally dried under vacuum to give **2 d**.

Procedure for the synthesis of MWNTs-supported catalyst 3 d

210 mg of **2 d** are dispersed in 100 mL of CH_2Cl_2 and the suspension is sonicated for 60 min. 31.5 mg of $[IrCp^*Cl_2]_2$ (0.038 mmol) is added and the reaction mixture is stirred for 48 h at room temperature. The suspension is filtered on a PVDF Millipore membrane (0.45 μm). The black solid is washed with 400 mL of THF, 400 mL of EtOH and 400 mL of Et_2O. The resulting powder is finally dried under vacuum to give **3 d.**

Procedure for the synthesis of MWNTs-supported catalyst 3d'

250 mg of *p*-MWNTs are dispersed in 100 mL NMP and the suspension is sonicated for 60 min. In parallel, a solution of 60 mg of **2 d'** (0.094 mmol, 1 eq.) in 10 mL NMP is prepared. The reaction mixture is stirred at 0 °C for 15 min before 0.5 mL of a 1 M HCl solution is added dropwise, 6.5 mg $NaNO_2$ (0.094 mmol, 1 eq.) is added as well and the reaction mixture is stirred 5 minutes at 0 °C. The solution color turns from yellow to orange. This solution is added to the nanotube suspension and the resulting mixture is stirred for 16 h at RT. The suspension is filtered on a PTFE Millipore membrane (0.22 μm). The black solid is washed with 400 mL DCM, 400 mL of EtOH and 400 mL of Et_2O. The resulting powder is finally dried under vacuum to give **3 d'**.

Catalysis

The general procedure for the hydroamination of A and C

The general procedure for the catalysed hydroamination A and C were undertaken by weighing the catalyst (1 mol% for **A**, 5 mol% for **C**) into a 2.5 mL thick-walled vial. To the solid catalyst, substrate (**A** or **C**, 0.06 mmol) and toluene-d_8 were added. Aliquots were taken at 1-, 2-, 5-, and 8-hour timepoints, and dissolved in 0.5 mL of toluene-d_8. When taking the samples, the vial was kept at room temperature, and the solid catalyst was allowed to settle. In cases where solid did not settle enough to allow for a homogeneous sample, the vial was centrifuged for 1 minute at 4000 rpm. The samples were monitored by ^{1}H NMR spectroscopy and the conversion (%) was determined by the relative integral ratios of selected ^{1}H resonances of the substrate and product(s).

For the recycling experiments, the reaction mixture was washed at the end of the reaction (8 hours) with 3×4 mL of toluene, and centrifuged. The vial was then recharged with **A** (0.06 mmol) and toluene (1 mL).

^{1}H NMR spectral analysis data for 1-pentynamine (**A**):

^{1}H NMR (400 MHz, $CDCl_3$): δ 2.84 (t, $^3J_{HH}$ = 6.9 Hz, 2H), 2.29 (td, $^3J_{HH}$ = 7.0; $^3J_{HH}$ = 2.7 Hz, 2H), 1.98 (t, $^4J_{HH}$ = 2.7 Hz, 1H), 1.76 (br s, 2H), 1.69 (tt, $^3J_{HH}$ = 7.0; 6.9 Hz, 2H).

^{1}H NMR (400 MHz, CD_2Cl_2): δ 2.75 (t, $^3J_{HH}$ = 6.9 Hz, 2H), 2.24 (td, $^3J_{HH}$ = 7.0; $^3J_{HH}$ = 2.7 Hz, 2H), 1.97 (t, $^4J_{HH}$ = 2.7 Hz, 1H), 1.61 (tt, $^3J_{HH}$ = 6.9 Hz, 2H), 1.28 (br s, 2H).

^{1}H NMR spectral analysis data for 1-pentynamine (**B**):

^{1}H NMR (400 MHz, toluene-d_8): δ 3.75 (m, 2H), 1.98 (m, 2H), 1.81 (br s, 3H), 1.69 (m, 2H).

^{1}H NMR spectral analysis data for 6-(2'-aminophenyl)hex-5-yn-1-ol (**C**):

^{1}H NMR (500 MHz, $CDCl_3$): δ 7.24 (dd, $^3J_{HH}$ = 7.9 Hz, $^4J_{HH}$ = 1.5 Hz, 1H), 7.07 (apparent td, $^3J_{HH}$ = $^3J_{HH}$ = 7.9 Hz, $^4J_{HH}$ = 1.5 Hz, 1H), 6.67 (dd, $^3J_{HH}$ = 7.8 Hz, $^4J_{HH}$ = 1.5 Hz, 1H), 6.65 (apparent td, $^3J_{HH}$ = 7.5 Hz, $^3J_{HH}$ = 7.8 Hz, $^4J_{HH}$ = 1.5 Hz, 1H), 3.71 (t, $^3J_{HH}$ = 6.3 Hz, 2H), 2.52 (t, $^3J_{HH}$ = 6.7 Hz, 2H), 1.79–1.69 (m, 4H).

^{1}H NMR spectral analysis data for 4-(1H-indol-2-yl)butan-1-ol (**D**):

^{1}H NMR (400 MHz, $CDCl_3$): δ 8.10 (br s, 1H, NH), 7.55 (d, $^3J_{HH}$ = 6.6 Hz, 1H), 7.29 (d, $^3J_{HH}$ = 7.2 Hz, 1H), 7.11 (m, 2H), 6.25 (s, 1H), 3.67 (t, $^3J_{HH}$ = 6.1 Hz), 2.76 (t, $^3J_{HH}$ = 7.4 Hz), 1.98 (br s, 1H, OH), 1.79 (apparent p, $^3J_{HH}$ = 7.0 Hz, 2H), 1.63 (apparent p, $^3J_{HH}$ = 7.4 Hz, 2H).

Acknowledgements

AD, SH and OR wish to thank the Fonds de la Recherche Scientifique (F.R.S.-FNRS), the Fonds pour la Formation à la Recherche dans l'Industrie et dans l'Agriculture (FRIA), as well as the Université catholique de Louvain for funding. They are also grateful to Jean-François Statsyns and François Billard for their technical assistance. IP and BAM wish to thank Macquarie University for infrastructural and funding support. IP would like to thank the University of Sydney for its infrastructural support and funding and would also like to thank Sydney Analytical.

Conflict of Interest

The authors declare no conflict of interest.

Keywords: Carbon nanotubes · Dendrimers · Hybrid catalysts · Hydroamination · Iridium catalysts

[1] M. K. Samantaray, V. D'Elia, E. Pump, L. Falivene, M. Harb, S. Ould Chikh, L. Cavallo, J.-M. Basset, *Chem. Rev.* **2020**, *120*, 734–813.
[2] C. Copéret, A. Comas-Vives, M. P. Conley, D. P. Estes, A. Fedorov, V. Mougel, H. Nagae, F. Núñez-Zarur, P. A. Zhizhko, *Chem. Rev.* **2016**, *116*, 323–421.
[3] T. J. Marks, *Acc. Chem. Res.* **1992**, *25*, 57–65.
[4] a) A. A. Tregubov, D. B. Walker, K. Q. Vuong, J. J. Gooding, B. A. Messerle, *Dalton Trans.* **2015**, *44*, 7917–7926; b) E. Ochoa, W. Henao, S. Fuertes, D. Torres, T. van Haasterecht, E. Scott, H. Bitter, I. Suelves, J. L. Pinilla, *Catal. Sci. Technol.* **2020**, *10*, 2970–2985; c) T. Wu, C. M. Fitchett, P. A. Brooksby, A. J. Downard, *ACS Appl. Mater. Interfaces* **2021**, *13*, 11545–11570; d) C. Queffélec, S. H. Schlindwein, D. Gudat, V. Silvestre, M. Rodriguez-Zubiri, F. Fayon, B. Bujoli, Q. Wang, R. Boukherroub, S. Szunerits, *ChemCatChem* **2017**, *9*, 432–439.
[5] a) H. Baydoun, J. Burdick, B. Thapa, L. Wickramasinghe, D. Li, J. Niklas, O. G. Poluektov, H. B. Schlegel, C. N. Verani, *Inorg. Chem.* **2018**, *57*, 9748–9756; b) S. Navalón, J. R. Herance, M. Álvaro, H. García, *Chem. Eur. J.* **2017**, *23*, 15244–15275; c) B. I. Kharisov, O. V. Kharissova, in *Carbon Allotropes: Metal-Complex Chemistry, Properties and Applications*, Springer International Publishing, Cham, **2019**, pp. 413–575; d) B. Moosa, K. Fhayli, S. Li, K. Julfakyan, A. Ezzeddine, N. M. Khashab, *J. Nanosci.* **2014**, *14*, 332–343.
[6] A. Peigney, C. Laurent, E. Flahaut, R. R. Bacsa, A. Rousset, *Carbon* **2001**, *39*, 507–514.
[7] a) S. Ruiz-Botella, E. Peris, *ChemCatChem* **2018**, *10*, 1874–1881; b) S. Sabater, J. A. Mata, E. Peris, *Organometallics* **2015**, *34*, 1186–1190.
[8] a) M. Blanco, P. Álvarez, C. Blanco, M. V. Jiménez, J. Fernández-Tornos, J. J. Pérez-Torrente, L. A. Oro, R. Menéndez, *ACS Catal.* **2013**, *3*, 1307–1317; b) C. Vriamont, M. Devillers, O. Riant, S. Hermans, *Chem. Commun.* **2013**, *49*, 10504–10506; c) S. C. Binding, I. Pernik, V. R. Gonçales, C. M. Wong, R. F. Webster, S. Cheong, R. D. Tilley, A. E. Garcia-Bennett, J. J. Gooding, B. A. Messerle, *Organometallics* **2019**, *38*, 780–787; d) M. Blanco, P. Álvarez, C. Blanco, M. V. Jiménez, J. Fernández-Tornos, J. J. Pérez-Torrente, J. Blasco, G. Subías, V. Cuartero, L. A. Oro, R. Menéndez, *Carbon* **2016**, *96*, 66–74.
[9] a) S. M. Grayson, J. M. J. Fréchet, *Chem. Rev.* **2001**, *101*, 3819–3868; b) J. López-Andarias, J. Guerra, G. Castañeda, S. Merino, V. Ceña, P. Sánchez-Verdú, *Eur. J. Org. Chem.* **2012**, *2012*, 2331–2337.
[10] a) D. Astruc, E. Boisselier, C. Ornelas, *Chem. Rev.* **2010**, *110*, 1857–1959; b) R. Esfand, D. A. Tomalia, *Drug Discov.* **2001**, *6*, 427–436; c) S. Svenson, D. A. Tomalia, *Adv. Drug Delivery Rev.* **2005**, *57*, 2106–2129; d) S. Mignani, J. Rodrigues, H. Tomas, M. Zablocka, X. Shi, A.-M. Caminade, J.-P. Majoral, *Chem. Soc. Rev.* **2018**, *47*, 514–532.
[11] a) D. Astruc, D. Wang, C. Deraedt, L. Liang, R. Ciganda, J. Ruiz, *Synthesis* **2015**, *47*, 2017–2031; b) D. Astruc, F. Chardac, *Chem. Rev.* **2001**, *101*, 2991–3024; c) D. Astruc, R. Ciganda, C. Deraedt, S. Gatard, L. Liang, N. Li, C. Ornelas, A. Rapakousiou, J. Ruiz, D. Wang, Y. Wang, P. Zhao, *Synlett* **2015**, *26*, 1437–1449.
[12] B. Helms, J. M. J. Fréchet, *Adv. Synth. Catal.* **2006**, *348*, 1125–1148.
[13] J. H. H. Ho, S. W. S. Choy, S. A. Macgregor, B. A. Messerle, *Organometallics* **2011**, *30*, 5978–5984.
[14] a) A. A. Tregubov, K. Q. Vuong, E. Luais, J. J. Gooding, B. A. Messerle, *J. Am. Chem. Soc.* **2013**, *135*, 16429–16437; b) C. M. Wong, D. B. Walker, A. H. Soeriyadi, J. J. Gooding, B. A. Messerle, *Chem. Sci.* **2016**, *7*, 1996–2004; c) C. Vriamont, M. Devillers, O. Riant, S. Hermans, *Chem. Eur. J.* **2013**, *19*, 12009–12017.
[15] a) A. Desmecht, T. Steenhaut, F. Pennetreau, S. Hermans, O. Riant, *Chem. Eur. J.* **2018**, *24*, 12992–13001; b) D. Sheet, A. Bera, Y. Fu, A. Desmecht, O. Riant, S. Hermans, *Chem. Eur. J.* **2019**, *25*, 9191–9196.
[16] a) K. Q. Vuong, C. M. Wong, M. Bhadbhade, B. A. Messerle, *Dalton Trans.* **2014**, *43*, 7540–7553; b) C. Hua, K. Q. Vuong, M. Bhadbhade, B. A. Messerle, *Organometallics* **2012**, *31*, 1790–1800.
[17] A. Desmecht, S. Hermans, O. Riant, *ChemistryOpen* **2017**, *6*, 231–235.
[18] M. Roemer, V. R. Gonçales, S. T. Keaveney, I. Pernik, J. Lian, J. Downes, J. J. Gooding, B. A. Messerle, *Catal. Sci. Technol.* **2021**, *11*, 1888–1898.
[19] A. Desmecht, D. Sheet, C. Poleunis, S. Hermans, O. Riant, *Chem. Eur. J.* **2019**, *25*, 1436–1440.
[20] A. Bonet, C. Pubill-Ulldemolins, C. Bo, H. Gulyás, E. Fernández, *Angew. Chem. Int. Ed.* **2011**, *50*, 7158–7161; *Angew. Chem.* **2011**, *123*, 7296–7299.
[21] a) M. Tavakkoli, M. Nosek, J. Sainio, F. Davodi, T. Kallio, P. M. Joensuu, K. Laasonen, *ACS Catal.* **2017**, *7*, 8033–8041; b) A. Maurin, M. Robert, *Chem. Commun.* **2016**, *52*, 12084–12087; c) M. Nosek, J. Sainio, P. M. Joensuu, *Carbon* **2018**, *129*, 175–182.
[22] a) A. Devadoss, C. E. D. Chidsey, *J. Am. Chem. Soc.* **2007**, *129*, 5370–5371; b) A. C. Gouget-Laemmel, J. Yang, M. A. Lodhi, A. Siriwardena, D. Aureau, R. Boukherroub, J. N. Chazalviel, F. Ozanam, S. Szunerits, *J. Phys. Chem. C* **2013**, *117*, 368–375.
[23] N. H. Metwally, G. R. Saad, E. A. Abd El-Wahab, *Int. J. Nanomed.* **2019**, *14*, 6645–6659.
[24] L. J. Fox, R. M. Richardson, W. H. Briscoe, *Adv. Colloid Interface Sci.* **2018**, *257*, 1–18.
[25] M. R. D. Gatus, I. Pernik, J. A. Tompsett, S. C. Binding, M. B. Peterson, B. A. Messerle, *Dalton Trans.* **2019**, *48*, 4333–4340.
[26] N. Sakai, K. Annaka, A. Fujita, A. Sato, T. Konakahara, *J. Org. Chem.* **2008**, *73*, 4160–4165.

Manuscript received: May 5, 2021
Revised manuscript received: July 26, 2021
Accepted manuscript online: August 4, 2021

FULL PAPERS

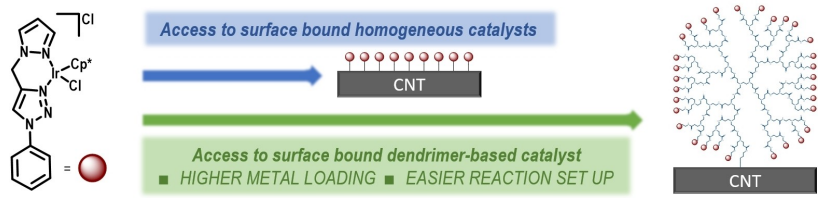

Dr. I. Pernik, Dr. A. Desmecht, Prof. B. A. Messerle, Prof. S. Hermans*, Prof. O. Riant**

One dendrimeric carbon nanotube surface-bound iridium(III) complex, and three analogous monometallic iridium(III) complexes were synthesised. These formed hybrid materials were tested as catalysts for hydroamination transformations to establish direct comparisons between the dendrimeric and monometallic systems.